

# Microfluidic Devices for Behavioral Screening of Multiple Zebrafish Larvae:

## Design Investigation Process

Arezoo Khalili<sup>1,#</sup>, Ellen van Wijngaarden<sup>1,#</sup>, Khaled Youssef<sup>1</sup>, Georg Zoidl<sup>2</sup>, Pouya Rezai<sup>1,\*</sup>

<sup>1</sup> Department of Mechanical Engineering, York University, Toronto, ON, CANADA

<sup>2</sup> Department of Biology, York University, Toronto, ON, CANADA

\* Corresponding Author: BRG 433B, 4700 Keele St, Toronto, ON, M3J 1P3, Canada; Tel: 416-736-2100 ext. 44703; Email: [prezai@yorku.ca](mailto:prezai@yorku.ca)

# Authors with equal contributions to this paper

## Keywords

Microfluidics, Zebrafish, Electrical stimulation, Behavioral screening, Multi-fish screening

## Abbreviations

dpf: days post fertilization

FOV: Field of view

RD: Response duration

TBF: Tail beat Frequency

TL: Tüpfel Long fin

## **Abstract**

Microfluidic devices have been introduced for phenotypic screening of zebrafish larvae in both fundamental and pre-clinical research. One of the remaining challenges for the broad use of microfluidic devices is their limited throughput, especially in behavioural assays. Previously, we introduced the tail locomotion of a semi-mobile zebrafish larva evoked on-demand with electric signal in a microfluidic device. Here, we report the lessons learned for increasing the number of specimens from one to four larvae in this device. Multiple parameters including loading and testing time per fish and loading and orientation efficiencies were refined to optimize the performance of modified designs. Simulations of the flow and electric field within the final device provided insight into the flow behavior and functionality of traps when compared to previous single-larva devices. Outcomes led to a new design which decreased the testing time per larva by approximately 60%. Further, loading and orientation efficiencies increased by more than 80%. Critical behavioural parameters such as response duration and tail beat frequency were similar in both single and quadruple-fish devices. The optimized microfluidic device has significant advantages for greater throughput and efficiency when behavioral phenotyping is required in various applications, including chemical testing in toxicology and gene screening.

## **1. Introduction**

Key characteristics of zebrafish, including transparency<sup>[1]</sup>, high genetic similarity to mammals<sup>[2]</sup>, small size<sup>[3]</sup> and quick growth<sup>[4]</sup> make it ideal for use in behavioral screening experiments<sup>[3,5]</sup> for disease and drug studies<sup>[6-8]</sup>. In contrast with cellular assays, working with organisms presents many challenges that severely limit their throughput<sup>[9]</sup>, particularly when it comes to behavioural investigations. Microfluidic devices have facilitated zebrafish tests,

enabling researchers to precisely manipulate, expose and monitor the larvae behaviours<sup>[10–12]</sup>. A wide variety of behavioural phenotypes associated with eye, fin, mouth and tail movements have been studied with microfluidic chips<sup>[13–16]</sup>. Studies using chemical<sup>[17]</sup>, electrical<sup>[14]</sup>, fluid flow<sup>[18]</sup> and light<sup>[19]</sup> to stimulate and assess various zebrafish behavioural responses have been reported.

Considering the hardships in stimulating the larva with accuracy using chemical, thermal and flow stimuli, and instabilities in their control, electrical stimulus can be considered as one of the best candidates because it can be turned on and off quickly and manipulated on-demand in terms of magnitude, direction and time. Moreover, mild electric signals have been shown not to affect small model organisms like *C. elegans* and zebrafish significantly<sup>[20,21]</sup>. However, the major challenge associated with the microfluidic chips previously developed to study the electric-induced behavioural responses of zebrafish larvae is their single-larva low throughput testing capability.

Until now, we have reported multiple microfluidic devices for monitoring the tail movement of individual zebrafish larvae in response to chemicals, fluid flow and electricity<sup>[13,14,18,21]</sup>. For instance, we demonstrated zebrafish larvae's preference to orient and swim directly toward the anode in a channel<sup>[21]</sup>. While freely swimming larvae can be studied in terms of overall movement, speed and travel distance, these experiments require greater device footprints and present difficulties in terms of quantification of subtle behavioural phenotypes. To address these limitations, we reported the on-demand response of semi-mobile (head trapped and tail free) zebrafish larvae to electrical stimulus in a confined microfluidic trap<sup>[14]</sup>. The electric-induced tail movement of the head-trapped larvae was quantified in terms of response duration (RD) and tail beat frequency (TBF) in the trap. It was demonstrated that an electric stimulus of 3  $\mu$ A produced the longest RD and the slowest TBF when currents between 1-9  $\mu$ A were tested.

1 Although the time and space required for testing a semi-mobile larva was reduced significantly  
2 compared to a freely moving larva, the challenge of long time required for behavioral screening  
3 of one larva at a time and resulting low assay throughput still remains unaddressed in this  
4 method.

5         Testing zebrafish individually in our semi-mobile assay involves a rest period in addition  
6 to the stimulus exposure time, summing the total length of an experiment to more than 100 s per  
7 zebrafish larva<sup>[14]</sup>. In this respect, increasing the number of zebrafish on the chip can reduce both  
8 the resting and stimulation times per fish. However, locomotor response testing requires  
9 zebrafish larvae to be spaced out on a device to allow complete tail strokes, while preventing tail  
10 collisions with the device walls. In combination with restrictions associated with the microscope  
11 field of view (FOV), this limits the number of larvae that can be tested simultaneously under a  
12 microscope. Loading multiple active zebrafish larvae individually into designated locations on  
13 the device and preventing them from escaping the device during the loading process pose  
14 challenges.

15         In this paper and through adapting experimental methods and modifying design  
16 components, we demonstrated that a multi-fish microfluidic device could be produced to reduce  
17 the time of behavioural screening and facilitate testing larger sample sizes with our electrical  
18 stimulation method. Much can be learned from the device design process described in this paper.  
19 Various methods of trapping and orienting the fish were investigated. Using finite element  
20 method, the impacts of the design modifications on the electric field (EF) and fluid flow through  
21 the device were examined. Our final design allowed us to (i) load four larvae in parallel into the  
22 device (restricted by microscope FOV), (ii) partially immobilize them with their heads trapped  
23 and tails moving in chambers, (iii) expose them to an on-demand electric stimulus and (iv)

quantify the electric-induced tail movements in terms of RD and TBF. Responses to electric stimulation were compared between the previously developed single-larva device and the multi-fish design to ensure the new device was fit for future testing. Our multi-fish device can be used in the future genetic and chemical screening assays for faster and more efficient research involving behavioural phenotypes of zebrafish larvae with potential applications in toxicology and drug discovery.

## **2. Materials and Methods**

### **2.1. Zebrafish Care**

Tupfel long fin (TL) zebrafish larvae between the ages of 5- and 7-days post fertilization (dpf) were used for testing of the microfluidic devices. Previously, we showed that the larvae's response to electric current at 5-7 dpf is similar<sup>[22]</sup>, so the age variation does not play a role in their response in this paper, which gives us a wider window of time for testing and minimizes sacrificing too many larvae. The fish were kept at 28 °C with a light to dark cycle of 14:10 hours. The swimming media used was an egg water solution with a concentration of 60 mg/ml instant ocean sea salt (Instant Ocean, Blacksburg, USA) and 0.1% methylene blue (M291-100 Fisher Scientific, USA). All experiments followed the necessary guidelines outlined by the Canadian Council for Animal Care (CCAC), based on Animal Care Committee (ACC) protocol GZ 2018-7 R2 and York University Biosafety Permit PR 02-19.

### **2.2. Microfluidic Device Fabrication**

Microfluidic devices tested in this paper were all fabricated from polydimethylsiloxane (PDMS). The master molds for PDMS casting were designed using the SolidWorks software

(SolidWorks Corp., USA) and printed using an Objet260 Connex3 printer (Stratasys Ltd., USA). Common components of the designs included an inlet, a main channel, larva trapping regions (TRs), screening pools and outlets. These components were carried over from our previous single-fish design<sup>[14]</sup> shown in Fig. 1A, and iteratively modified for multi-fish screening.

Our single-fish design was used as a reference device and consisted of three layers with the inlet, outlet, main loading channel, electrodes, TR and screening pool contained within the top layer. The bottom layer contained a L-shaped valve channel that could be pressurized with air to cause a middle PDMS membrane to deflect upwards at the intersection of the valve and the main loading channel and create a physical barrier in front of the trapped zebrafish larva to prevent its escape from the TR. Several modifications including altered trap dimensions and alternative loading and orientation techniques were considered to design a novel device, enabling simultaneous behavioral screening of four fish in this paper.

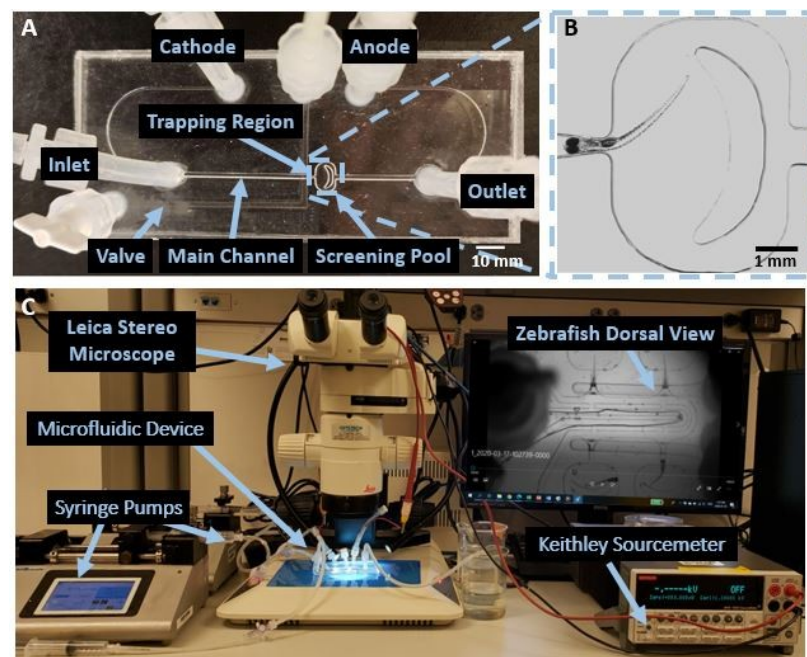


*Fig. 1. A previously-reported single-fish device for screening the electric-induced response of semi mobile 5–7 dpf zebrafish larva. A) The device consisted of an inlet, an outlet, a larva trapping region, a*

1 *tail screening pool and interconnecting channels to two end reservoirs with electrodes. B) Close-up view*  
2 *of screening pool and a larva trapped in the TR. C) Experimental setup to test microfluidic devices for*  
3 *behavioural screening of zebrafish larvae, with the main equipment including two syringe pumps,*  
4 *microscope, electrical sourcemeter, and a computer.*

5 Printed molds were first thoroughly cleaned with soap and water to remove any support  
6 material. A 10:1 ratio of PDMS base to curing agent was thoroughly mixed and air bubbles were  
7 removed using a vacuum chamber. After pouring the PDMS pre-polymer into the mold, the  
8 device was allowed to cure on a hotplate at 50 °C<sup>[23]</sup>. Once fully cured after approximately 6 hr,  
9 the PDMS layer was removed from the mold and plasma bonded to glass or additional layers of  
10 PDMS to produce the final device. This final step was completed using a plasma bonder (PDC-  
11 001-HP, Harrick Plasma, USA) for surface activation and bonding of the layers.

### 13 **2.3. Experimental Setup and Procedure**

14 As shown in Fig. 1C, the experimental setup consisted of a Leica upright microscope  
15 (Stereomicroscope Leica MZ10F, Singapore), digital C-mount camera (GS3-U3-23S6M-C, Point  
16 Grey Research Inc., Canada), one of the designed microfluidic devices, the necessary number of  
17 syringe pumps based on the device design (LEGATO 111, KD Scientific Inc., USA) and tubing  
18 to connect to the device. An electric source-meter (Model 2410, Keithley, USA) was attached to  
19 the electrodes of the device to supply electric stimulus during behavioural screening.

20 To conduct an experiment, the required number of zebrafish larvae, at the age of 5-7 dpf,  
21 were loaded into the main loading channel via the inlet of the device using a volumetric flow rate  
22 of 1 ml/min. The larvae were directed into the TRs and partially immobilized such that their tails  
23 could still move freely in the adjoining screening pools (e.g. Fig. 1B). When any valve channels

situated in the bottom layer were pressurized, the membrane deflected, creating a physical barrier in the intersecting upper layer channels. This provided a way to prevent the larvae from swimming out of the TR. A period of 60 s was provided to allow the fish to adjust to the new environment and recover from the loading process.

Several modifications in the size and shape of the traps were applied to enable loading multiple larvae simultaneously. Different loading and orientation strategies from addition of an orientation loop to indirect flow assisted loading were also considered to increase the number of larvae tested at the same time. To assess the functionality of our proposed designs, 10 trials were conducted in each design resulting in sample sizes between 10-40 fish depending on whether the design was for a one, two or four zebrafish. The tests provided an understanding of the design deficiencies. To compare the functionality of different designs, the testing time per fish, loading efficiency and orientation efficiency of each design was calculated using Eq. (1), (2) and (3), respectively.

$$\text{Testing time per fish} = \frac{\text{Loading time} + 60 \text{ s recovery period} + 20 \text{ s stimulation interval}}{\text{Number of fish successfully oriented} \in \text{the device}} \quad (1)$$

$$\text{Loading efficiency} = \frac{\text{Number of larvae trapped} \in \text{the TRs}}{\text{Number of TRs} \in \text{the device}} \quad (2)$$

$$\text{Orientation efficiency} = \frac{\text{Number of fish correctly positioned} \in \text{the TR (with tails} \in \text{the screening pool)}}{\text{Total number of larvae trapped}} \quad (3)$$

The final successful design in loading was then modified to include electrodes to apply the required electrical stimulus for behavioural assays. Recordings were used to find the electric-induced RD and TBF of zebrafish larvae (Eqs. 4, 5) to characterize the tail movement. Lastly, these recordings and the data yielded from testing were further analyzed using statistical analysis.



$$Response\ Duration(RD) = Movement\ End\ Time - Movement\ Start\ Time \quad (4)$$

$$Tail\ Beat\ Frequency(TBF) = \frac{Number\ of\ full\ tail\ cycles}{RD} \quad (5)$$

#### 2.4. Numerical Model

The model of the final device design was created using SolidWorks (SolidWorks Corp., USA) and imported into COMSOL Multiphysics (COMSOL Inc., Sweden) for three-dimensional (3D) simulations of the device. Generally, the device consisted of an assortment of traps connected through the inlet and outlet reservoirs, where the electrodes were inserted.

The electric current module in COMSOL was applied to determine the required total electric current at the electrodes in the final device so that each fish was exposed to the electric current of 3  $\mu$ A, as was the case in our previous single-fish device<sup>[14]</sup>. The EF within a conductive media was modeled by solving Ohm's law (Eq. 6) using the steady-state direct-current electric module. Both Eqs. (6) and (7) were applied to map the voltage distribution and current density. In these equations,  $J$ ,  $\sigma$ ,  $E$ ,  $D$ ,  $\epsilon_0$  and  $\epsilon_r$  represent the current density, material conductivity, EF, electric displacement field, permittivity of free space and relative permittivity.

$$J = \sigma E \quad (6)$$

$$D = \epsilon_0 \epsilon_r E \quad (7)$$

The electric conductivity of tap water was determined using the conductivity measurement kit (Combo meter (HI98129), HANNA instruments, Italy). The values of 50 $\Omega$ , 293.15K, 0.034 S/m, and 80 were defined for the reference impedance, temperature, electrical conductivity and relative permittivity, respectively. The device outlets positioned downstream of

the TRs were set as anodes while a central channel boundary upstream from TRs was set to cathode. All other channel boundaries were defined as electric insulation.

COMSOL was also used for a flow field simulation to understand the fluid behavior and its correlation with the experiment in terms of flow patterns and fish loading sequence in the traps. The laminar flow module was applied and the relevant boundary, initial, and material conditions were defined. The Navier-Stokes (Eq. 8) and the continuity (Eq. 9) equations were used for the conservation of momentum and mass, respectively. The fluid was regarded as incompressible and Newtonian with gravity forces and viscous dissipation effects neglected in the equations.

$$\rho(u \cdot \nabla)u = \nabla \cdot [-pI + \mu(\nabla u + (\nabla u)^T)] \quad (8)$$

$$\rho \nabla \cdot u = 0 \quad (9)$$

The variables  $\mathbf{u}$ ,  $p$ ,  $\rho$ , and  $\mu$  are the velocity vector, pressure, density, and dynamic viscosity, respectively. An inlet flow rate of 1 ml/min and an indirect flow rate of 0.8 ml/min was inputted to reflect the values implemented during the experiments. While the inlets were described in terms of volumetric flow rates, the outlets were set to atmospheric pressure. The media was defined as water and a no-slip condition was added to all channel walls.

Mesh independency was checked for both electric and flow simulations to ensure accuracy as described in the Supplementary File section S1.

## 2.5. Viability Test

Finalizing the design, a viability test was done on larvae following procedures reported by Peimani et al.<sup>[21]</sup> to confirm that the fish were not injured by the loading technique, the device components and the electrical stimulus. The morphology and survival criteria were applied to

examine the immediate and long-term impacts of the loading, immobilization and electric stimulation processes. Three groups of larvae were tested (N=20 fish in three independent trials), including a reference group that was neither exposed to the device nor to any electric current, a control group with larvae trapped in the device for 80 s but not exposed to any electric current, and a test group of larvae exposed to electric current (at 3  $\mu$ A in each trap) for 20 s inside the device. For gauging survival and morphological abnormalities, the fish were unloaded from the device through the tilted inlet tube, using the withdrawal function of the syringe pump and their viability and morphology was assessed each day over a period of 10 days. This approach reduced the chances of damaging the larvae as they were being removed from the device for the subsequent tests. Morphology criteria included craniofacial abnormalities and bending (i.e. scoliosis, kyphosis, and lordosis)<sup>[24,25]</sup> as described in Supplementary File section S2.

## **2.6. Data Analysis**

Various statistical tools were applied during the analysis phase to aid with extracting meaningful information from the tests. The mean, median, and minimum and maximum data values were provided in box plots, offering a clear depiction of the data distribution and interquartile ranges. Errors were described using the Standard Error of the Mean (SEM). The data were tested for normality using Shapiro-Wilk test. Then, relying on Shapiro-Wilk test outcome, Mann–Whitney U test was used to ascertain if significant differences were present. The sample sizes were determined using power analysis with an upper limit of 0.05 and a significance level of 80%.

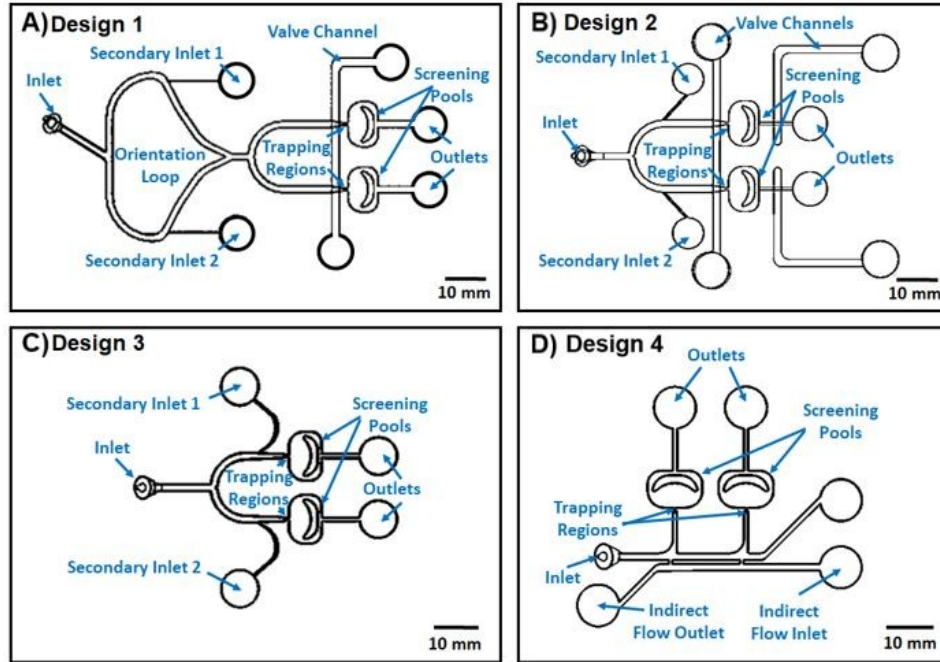
## **3. Results and Discussion**

We first examined various designs for proper loading and orientation of two zebrafish larvae in parallel head-trapping regions in multiple microfluidic devices. Design iterations were compared using parameters such as the loading and orientating success. The optimum double-fish design configuration was then assessed following the viability test protocol mentioned in the Materials and Methods section, and expanded to develop a device for partial immobilization and behavioral screening of four zebrafish larvae in parallel, restricted by our microscope's FOV and the space needed for larvae's full tail oscillation. Using COMSOL simulation, numerical analysis was applied to understand the EF condition in the device and to ensure that a consistent electric stimulus will be applied in all trapping regions for testing multiple larvae. Flow simulation was also used to demonstrate that the device did not harm the zebrafish larvae during the loading process as the maximum shear stress observed was well below the threshold defined in the literature<sup>[26,27]</sup>. We also examined the viability of the zebrafish larvae in our quadruple-fish device before quantitative comparison of devices in terms of loading time per fish, loading efficiency, orientation efficiency, testing time per fish, and last but not least, the RD and TBF of zebrafish larvae. The experiments provided valuable design insights pertaining to fabrication and the overall user friendliness of device operation, along with quantitative data about behavioral response of zebrafish larvae to electric signal in microfluidic channels.

### **3.1. Orientation and Head-Trapping of Two Zebrafish Larvae Investigated in Multiple Microfluidic Device Designs**

To achieve trapping of two zebrafish larvae from their heads in parallel TRs of a single device, our original design shown in Fig. 1A-B was modified four times as shown in Fig. 2, and

1 each design was compared in terms of the proper loading and orientation of the larvae in the  
2 traps.



3  
4 *Fig. 2. Different designs tested for the optimization of the double-fish microfluidic device. A) Design 1:*  
5 *double fish device with orientation loop, B) Design 2: double fish device with valves, C) Design 3: double*  
6 *fish device with modified trap, and D) Design 4: double fish device with indirect flow assisted loading.*

### 7 3.1.1. Design 1: Double-Fish Device with Orientation Loop

8 As the most obvious iteration, Design 1 in Fig. 2A was created to investigate if a trap  
9 similar to the one previously reported for single-larva studies<sup>[14]</sup> in Fig. 1A could be used twice in  
10 parallel to load two fish into the device. Therefore, some similar features including the trap,  
11 screening pool, valve layer, inlet and channel dimensions were applied in Design 1. The TR  
12 which is shown in Fig. 3A was gradually narrowed in width, from 0.9 to 0.25 mm, to mimic the  
13 ergonomic structure of 5-7 dpf zebrafish larvae from head to the yolk region. Considering the  
14 idea of direction-switching loop reported by Lin et al.<sup>[15]</sup>, an orientation loop was added

1 downstream of the inlets to allow for the fish to be directed by flow towards the TR with their  
2 tails facing the trap (tail-first). If a larva was loaded head-first, flow from the secondary inlet 2  
3 would push the larva into the TR as seen in supplementary video V1. Otherwise (for a tail-first  
4 larva), the secondary inlet 1 would be involved to move the larva into the TR.

5 We fabricated the device and conducted 10 trials with 2 larvae per trial (N=20). This  
6 design was not successful in either orientation or trapping the larvae. Loading the first larva was  
7 easy but the trap size was not suitable to hold the fish in place while the second larva was being  
8 loaded. In most of the cases, the first larva was ejected from the device while the second larva  
9 was being loaded. Moreover, fish were able to turn at different intersections, rendering the idea  
10 of orientation loop ineffective in our device as shown in supplementary video V2. Due to these  
11 difficulties, this design was rejected in our studies.

### 13 3.1.2. Design 2: Double-Fish Device with Valves

14 Design 2 in Fig. 2B was developed to address the Design 1 issues of the fish being  
15 washed through the traps during loading and controlling the orientation of the larvae. In Design  
16 2, we utilized a second deflectable PDMS membrane valve downstream from the screening pools  
17 to block the flow and prevent the fish from being washed through during the loading process.  
18 The orientation loop was also removed, and the secondary inlets were shifted to minimize the  
19 number of junctions and opportunities for the larvae to rotate in the channel. In this case, the  
20 secondary inlets were positioned as shown in Fig. 2B to direct the larvae into the proper trap  
21 based on their longitudinal orientation direction in the U-shaped channel. For example, for a  
22 larva loaded in the top branch with its head facing toward the TR, flow from secondary inlet 1  
23 was used to send the larva into the bottom TR.

A total of N=20 zebrafish larvae were tested in 10 trials in this device. The additional valves could not completely cut off the channels, letting a small flow pass through the TR which was enough to push the zebrafish larva out of position. Moreover, actuating the additional valves added to the difficulty of loading and consequentially increased the loading time. Removing the orientation channel shortened the inlet channel and decreased the user friendliness of the device as orientating the fish had to be done in a smaller section. Although the secondary inlets offered sufficient control to position the fish into the desired trap, it proved time consuming to operate and adjust the flow rate based on the position of the larvae. Accordingly, Design 2 was also abandoned in our studies.

### *3.1.3. Design 3: Double-Fish Device with Modified Traps*

In the original device shown in Fig. 1A and in both Designs 1 and 2 of the double-fish devices, the trap design remained unaltered as shown in Fig. 3A. Preliminary experiments in the double-fish devices presented difficulties in maintaining the larvae in these traps as discussed above. Therefore, Design 3 in Fig. 2C specifically targeted the issue of the fish being washed through the device during loading. The valve layer in Design 2 was removed, and the focus of the design was put on shaping the traps to find the size that would hold the zebrafish larvae securely. The device used the same secondary inlet channels to reduce the number of factors that were changing from the previous design. However, we utilized longer channels to facilitate loading, with the secondary inlets pushed farther back along the U-shaped main channels.

The original trap shape in the single-larva device and Designs 1 and 2 had a rectangular cross-section with a width of 0.25 mm and a height of 0.55 mm (Fig. 3A). In Design 3, three trap shapes were tested consecutively, i.e. a half-oval shape (0.25 mm diameter by 0.25 mm height), a

semicircular design ( $r = 0.15$  mm) and a rectangular design (0.25 mm width by 0.4 mm height) as shown in Fig. 3B-D, respectively. The overall shape and dimensions were adjusted based on the average measurements of 5-7 dpf larvae's heights and widths.

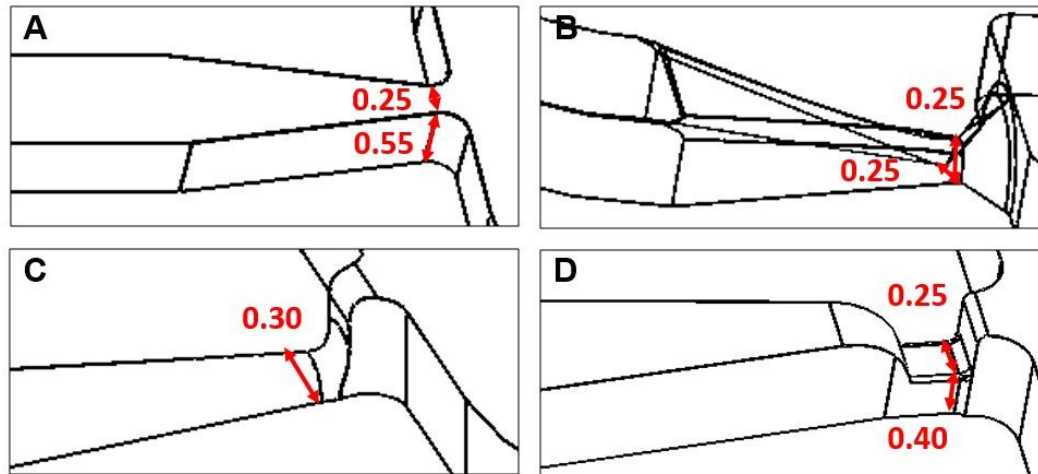


*Fig. 3. Close up views of trap designs for A) the original single-larva device and Designs 1-2, B) Design 3 with oval trap, C) Design 3 with semicircular trap, and D) Design 3 with rectangular trap (which was the most successful and also applied to Designs 4-5).*

Both the semicircular and ovular trap shapes in Fig. 3B and 3C were observed to trap the fish very tightly appearing to place undo stress on the fish. The rounded geometry resulted in the fish acting like a plug and blocking flow completely increasing the pressure drop experienced by the fish in the trap. The final rectangular shaped trap in Fig. 3D proved effective in holding the fish in the TR while allowing a small amount of flow around the fish as shown in supplementary video V3.

A viability test was done to confirm that the fish were not affected by the loading technique and the device components in Design 3. During the 10 days of post-assay monitoring, the survival rates of the control (exposed to device flow) and the reference (not exposed to



device) groups were similar (Fig. S3A, Mann-Whitney U test,  $p\text{-value} > 0.05$ ). More than 86% of the fish loaded into the device showed a normal morphology, demonstrating no significant difference with the reference group (Fig. S3B, Mann-Whitney U test,  $p\text{-value} > 0.05$ ). In summary, we concluded that the loading and trapping operations in Design 3 did not have a significant adverse effect on the zebrafish larvae.

While the modified TR proved effective in trapping the fish, controlling the orientation remained challenging. Although secondary inlets enabled efficient trapping, sufficient time and expertise was required to adjust the flow rates from the main and secondary inlets to position the larvae in a tail-first orientation. The trap shape was deemed suitable for use in subsequent designs and the focus was shifted to addressing the fish orientation.

#### *3.1.4. Design 4: Double-Fish Device with Indirect Flow Assisted Loading*

To achieve tail-first orientation for the larvae, various methods were considered ranging from altering the previously unsuccessful orientation loop (Design 1) to the use of secondary inlets (Designs 2 and 3), and finally applying EF for orientation before loading the larvae into the traps (results not reported). The challenges associated with Designs 1-3 were already discussed in the previous sections. The use of electric stimulus to orient the fish was ruled out due to the possibility of adaptation to the EF<sup>[28]</sup> or altering the electrically induced movement response, which we aimed to test with the final optimized design.

In Design 4, an indirect flow assisted loading technique inspired by the work of Lin et al.<sup>[15]</sup> was used. The indirect flow was used to facilitate the loading and trapping procedure (Fig. 2D). Once the larvae were loaded, the flow velocity was adjusted so that rheotaxis<sup>[18]</sup> ensured tail-first orientation for the majority of the trials. Additionally, the width of the main channel was

decreased from 0.9mm to 0.8mm to decrease the possibility of larvae's turning at the junctions. The indirect flow was run in the opposite direction parallel to the main channel and was connected with the main channel through a series of short vertical channels (0.2 mm wide and 0.55 mm deep). Water was pumped into the main channel through these vertical channels to increase the hydrodynamic flow focusing on each trap and preventing the larva from swimming back. A trapped larva could act as a partial plug, raising the flow resistance in the first trap and directing the main flow to the second trap. Consequently, the second larva bypassed the occupied trap and was carried into the next TR.

Testing N=20 larvae, the success of Design 4 in regard to loading, orientation and trapping made it more appealing than Design 3 as seen in supplementary video V4. This design was modified further (see next section) to increase the number of fish being tested simultaneously, reduce the testing time per fish, and make full use of the microscope field of view.

### **3.2. Design 5: Quadruple-Fish Device with Indirect Flow Assisted Loading**

Design 5 in Fig. 4 was created to investigate the possibility of expanding the indirect flow loading and trapping method in Design 4 (Fig. 2D) for testing of four zebrafish larvae simultaneously. Design 4 was expanded with screening pools and traps arranged to fit under our microscope FOV of 12 mm by 18 mm. The main channel width was also further reduced to 0.7 mm to reduce the capability for the larvae to turn at the intersections. Additionally, a valve layer in front of the TR was added to prevent the fish from swimming back into the main channel when the indirect flow was switched off, similar to the valve channel used in the single-fish device.

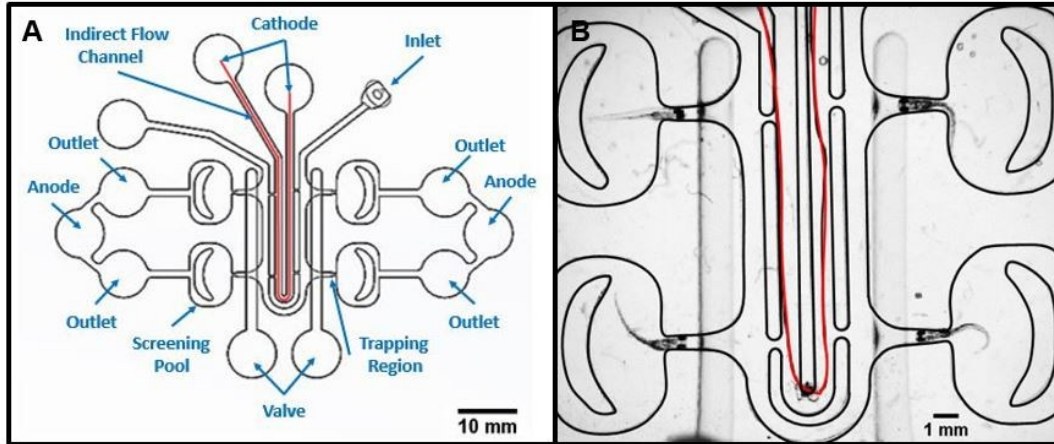


Fig. 4. Design 5: Quadruple-fish device with indirect flow assisted loading. A) Model of the device showing the inlets, outlets, screening pools, valve channels and electrodes. B) The fabricated device with four zebrafish larvae loaded into the TRs. The cathode electrode running through the indirect flow channel is shown in red.

Loading was accomplished using flow rates of 1 ml/min and 0.8 ml/min in the main and indirect flow channels, respectively. This process resulted in successful orientation and trapping of four larvae as shown in Fig. 4B and supplementary video V5. The loading trials (N=40) proved that the design was ready to move to the next stage of modifications for electrical stimulation and behavioral testing of the loaded larvae. The design was modified accordingly to include locations for the electrodes with a wire running through the indirect flow channel (shown in red in Fig. 4) to act as the cathode and outlets being added for the anode wires.

### 3.2.1. Viability Test of Larvae in the Quadruple-Fish Device

Viability and morphological testing were repeated in our quadruple-fish device to ensure that electric stimulation would have no significant impact on the zebrafish. Three groups of larvae including a reference group (kept off-chip), a control group (exposed to device flow only)

and a test group (exposed to device flow and EF) were tested. During the 10 days of post-experimental monitoring, the survival rates of all three groups were similar (Fig. S4A, two-tailed t-test,  $p\text{-value} > 0.05$ ). More than 85% of the fish exposed to the device or the electric current did not show any abnormal morphology, showing statistical similarity with the reference group (Fig. S4B, two-tailed t-test,  $p\text{-value} > 0.05$ ). Therefore, we concluded that the device and electric stimulation did not have any significant effect on the zebrafish larvae in the quadruple-fish device.

### 3.2.2. Numerical Analysis of the Quadruple-Fish Device

Design 5 was further analyzed using electric and flow simulations to ensure similar electro-fluidic conditions for all fish trapped in the TRs. For details on the model and mesh independency, please refer to the Materials and Methods section and the Supplementary file section S1, respectively. Previous experiments in our single-fish device (Fig. 1A) used an electric stimulus of  $3\text{ }\mu\text{A}$  to induce tail movement<sup>[14]</sup>. As shown in Fig. 5A, we achieved a uniform voltage drop of 1.1 V in each trap along the cut lines A-A', B-B', C-C' and D-D' (displayed in the upper right corner of Fig. 5B) by applying a total electric current of  $12\text{ }\mu\text{A}$  between the electrodes of the Design 5 device. Fig. 5B demonstrates the current density in traps A-D. Overlapping the four graphs confirmed that the current density across all traps was the same. An electric current of  $3\text{ }\mu\text{A}$ , consistent with that used in our single-fish device, was obtained across each trap when the current density was multiplied by the area of the channel along the cutline at any given point<sup>[14]</sup>.

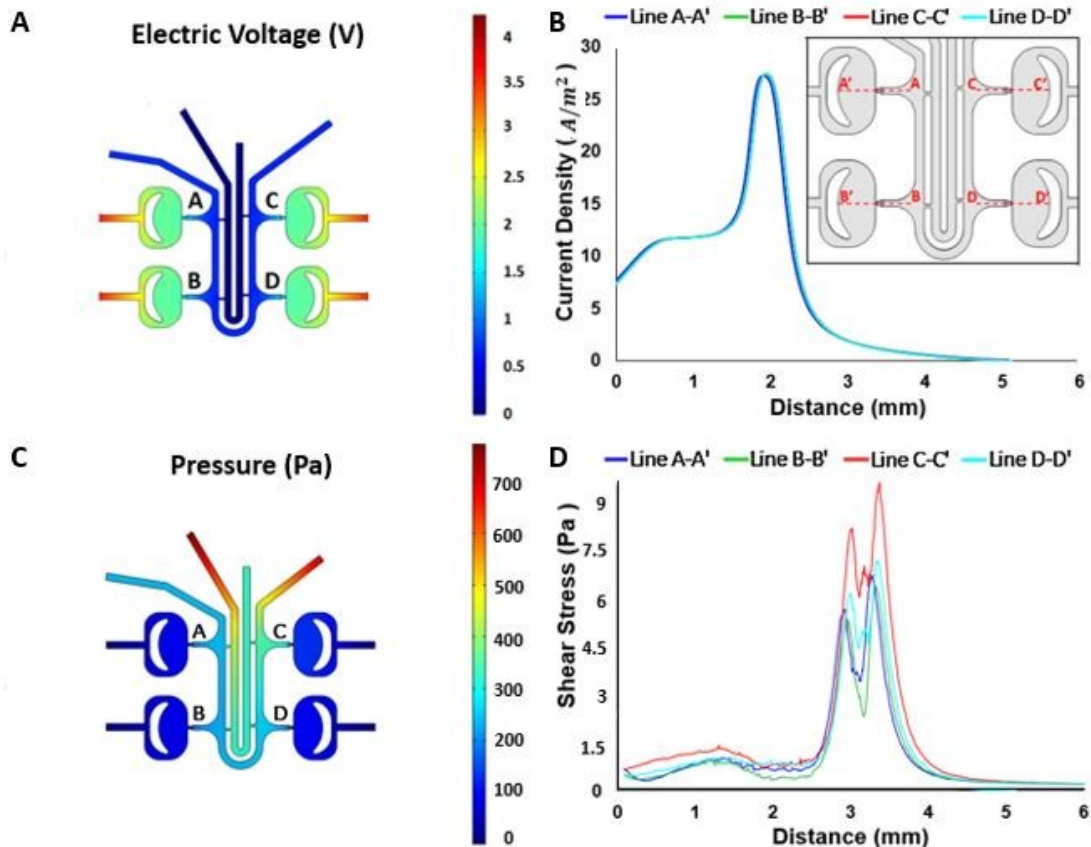


Fig. 5. COMSOL simulation results of A) the electric voltage and B) current density within the chip (Design 5) before larvae loading, indicating a uniform voltage and current in all four traps. C) Fluid pressure magnitude and D) shear stress magnitude within the chip during loading.

Flow simulations were performed to understand the pressure, shear stress, and flow distribution in the channel and to predict the trap loading sequence. The pressure magnitude and shear stress were plotted to ensure uniform loading conditions in TRs (Fig. 5C and 5D). Simulation results in Fig. 5C for the flow dynamics within the chip indicated a pressure drop and hence a hydrodynamic force pointing from the main channel towards the traps that was utilized to load and immobilize the zebrafish larvae. The change in pressure for traps A to D were found along the cut lines of A-A' to D-D'. The pressure drop magnitudes were 152 Pa, 145 Pa, 215 Pa and 160 Pa for Traps A, B, C and D, respectively, as shown in section S5 of the supplementary

file. This sequence was perfectly matched with the larvae loading patterns observed during experiments validating the simulation (supplementary video V5). Trap C was always loaded first, due to the significantly larger pressure drop, while some variation in the loading order could be seen between the three other traps likely due to the similarity in pressure drop values.

The water viscosity was multiplied by the velocity gradient at the wall to obtain the shear stress in the traps in Fig. 5D. Shear stress varied along the narrowing traps due to the altered flow velocity, which was compared to the levels of stress known to damage the larvae. Studies done by Ulanowicz and Morgan<sup>[26,27]</sup> examined the effects of shear stress due to fluid flow on various fish species at the egg, larval and fully developed stages. The maximum shear stress to avoid injury in larval fish was found to be approximately 45 Pa. This far exceeded the maximum shear stress of less than 10 Pa that the zebrafish experienced during loading in our device (Fig. 5D).

### 3.3. Quantitative Comparison of Single-, Double- and Quadruple-Fish Designs

To compare the effectiveness of various devices, the four key designs were considered including the single-fish device (Fig. 1A)<sup>[14]</sup>, the double-fish devices with modified traps (Design 3 in Fig. 2C) and the indirect flow assisted loading (Design 4 in Fig. 2D), as well as the quadruple-fish device with indirect flow loading (Design 5 in Fig. 4). Running 10 tests in each device resulted in sample sizes ranging from 10 to 40 fish (10 fish in the single, 20 in the double and 40 in the quadruple designs). The loading times per fish were  $30 \pm 3.7$  s,  $28.9 \pm 3.7$  s,  $26.9 \pm 2$  s and  $20.4 \pm 4.1$  s for the four Designs, respectively (Fig. 6A), with no significant difference found between the loading times (Mann-Whitney U test, p-value > 0.05). Statistically similar loading efficiencies of  $85 \pm 7.6\%$ ,  $85 \pm 7.6\%$  and  $87.5 \pm 5.6\%$  were obtained for Designs 3, 4 and 5, respectively (Mann-Whitney U test, p-value > 0.05) (Fig. 6B). Since, the same loading strategy

and trap design was used in all three devices, similar loading times and efficiencies could be expected. Comparing the orientation efficiencies clarified the advantage of Design 4 over 3. Using Design 4, we could achieve an orientation efficiency of  $90\pm7.1\%$  that was significantly higher than Design 3 (Mann-Whitney U test,  $p\text{-value} > 0.05$ ,  $p\text{-value} < 0.05$ ). Therefore, the same orientation technique used in Design 4, was employed in Design 5 to trap four zebrafish larvae.

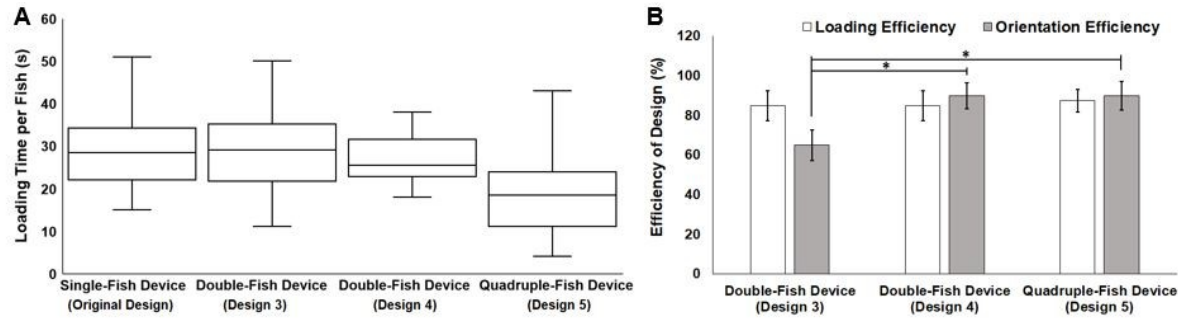


*Fig. 6. Performance comparison of different devices, showing the A) loading time per fish and the B) loading and orientation efficiencies. The lines within the boxes mark the median. Upper and lower boundaries are the 75<sup>th</sup> and 25<sup>th</sup> percentile and whiskers are the maximum and minimum. Error bars are SEM. N=10, 20, 40 for single-, double- and quadruple-fish devices, respectively.*

To assess the competitive value of quadruple-fish device over the other three devices, the total testing time per fish in each device was calculated and compared in Fig. 7. Testing times of  $110\pm3.7$  s,  $80.9\pm9.3$  s,  $78.9\pm6.7$  s and  $44.4\pm4.8$  s were found for the single-, double- (Design 3 and Design 4) and quadruple-fish devices, respectively. Fig. 7 shows a significant decrease in the testing time per fish as we move from single- to double-fish devices, as a result of the design alterations. The testing time was further reduced in the quadruple-fish device by approximately 60% compared to the single-fish device.

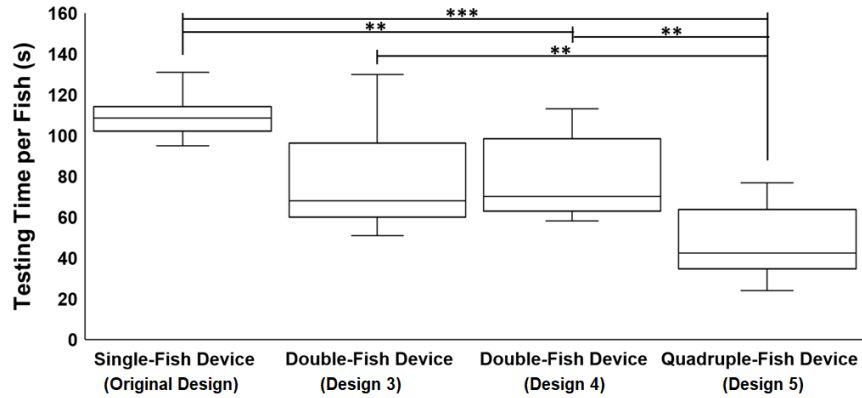


Fig. 7. Comparison of total testing time per fish for the landmark devices. The lines within the boxes mark the median. Upper and lower boundaries are the 75<sup>th</sup> and 25<sup>th</sup> percentile and whiskers are the maximum and minimum. \*\*:  $p < 0.01$ , \*\*\*:  $p < 0.001$ .  $N=10, 20, 40$  for single-, double- and quadruple-fish devices, respectively.

### 3.4. Locomotor Response in Single and Quadruple-Fish Devices

As the single-fish device has already been established<sup>[14]</sup>, the RD and TBF of fish tested in the quadruple-fish device was compared with those in the single-fish device for validation purposes. The total electric current of 12  $\mu\text{A}$  (3  $\mu\text{A}$  per trap) obtained through the electric-field simulation in COMSOL was applied in the quadruple-fish device, while an electric current of 3  $\mu\text{A}$  was used in the single-fish device, ensuring the larvae were exposed to a consistent stimulus in all traps in both devices.  $N=45$  larvae in three trials were tested and the results in Fig. 8 indicate that no significant change was found in the electric-induced responses in the two devices. The RDs and TBFs were statistically similar among the devices, based on a Mann–Whitney U with  $p\text{-value} > 0.05$ . Therefore, the final device enables testing of four fish simultaneously without altering the locomotor response while reducing the time of experiment significantly. As the stimulus must be applied only once to the four zebrafish larvae, the new platform facilitates larger sample sizes and offers a way to make screening more efficient. In



addition to this, the final device offers a uniform testing environment, ensuring factors such as stimulus duration and magnitude are the same for all fish.

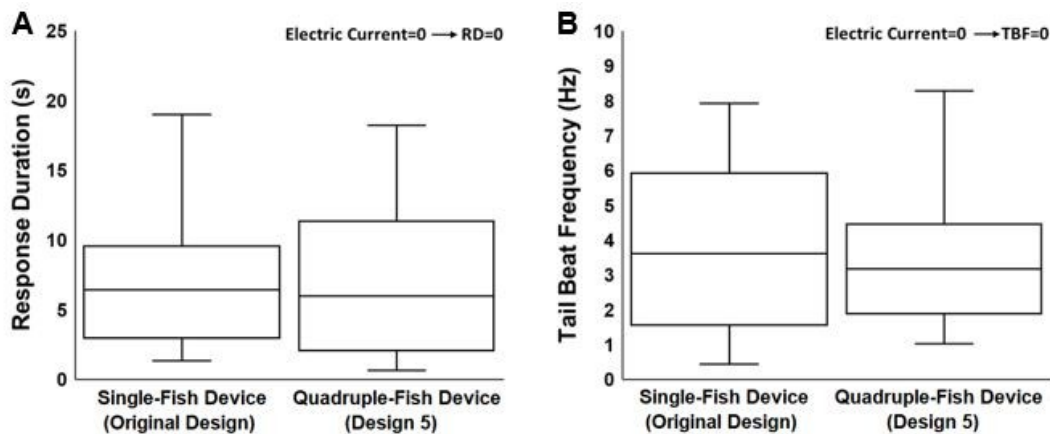


Fig. 8. A) Response duration and B) tail beat frequency of zebrafish larvae exposed to electric current of  $3 \mu A$  inside the single-fish and the quadruple-fish devices. The lines within the boxes mark the median. Upper and lower boundaries are the 75<sup>th</sup> and 25<sup>th</sup> percentile and whiskers are the maximum and minimum.  $N=45$  per experimental condition in three independent trials.

## 4. Conclusion

An effective microfluidic device for decreasing the testing time of behavioural assays of 5-7 dpf zebrafish larvae was demonstrated. The device provided a convenient platform for manipulation, testing and imaging four zebrafish larvae simultaneously for tail movement screening. The first step in the design process involved correctly orienting and successfully trapping larvae for screening. Investigating various trap shapes and valve configurations, we ended up with the final rectangular cross-section dimensions to successfully hold the fish in a dorsal position within the traps. Different methods for longitudinal orientation of larvae were researched including using an orientation loop, direct flow and indirect flow. The final design's

use of indirect flow for loading provided the loading and trapping efficiencies of 87.5% and 90%, respectively and offered sufficient control for experiments.

Simulations were utilized to ensure that the device was suitable for behavioural screening. The numerical simulation of the EF was used to find the required current stimulus and verify that a uniform EF for each trap-screening pool configuration was obtained. Flow simulations providing the pressure drop across the trap and the shear stress matched the fish loading sequence seen during experiments and ensured that the maximum stress applied was below the threshold for damaging larvae. A viability test was conducted in addition to the numerical tests to ensure the fish are not injured. These results provided further evidence that the device was suitable for use. No difference in RD and TBF for the quadruple-fish device and single-fish device were found, while the testing time per fish was reduced by approximately 60%. The presented design is, therefore, ideal for future behavioral, genetic and chemical screening assays of multiple zebrafish larvae.

The demonstrated techniques and design will enable faster and more efficient screening, holding potential in the fields of phenotypic neurobehavioral research for drug discovery and toxicology. Further modifications to the device, dependent on the microscopy capabilities such as the FOV, could increase the number of fish tested simultaneously to further reduce the testing time and enhance the throughput of behavioral assays with the proposed technology.

## Acknowledgments

This research was made possible through the funding received from the Ontario Early Researcher Award to PR, Brain Canada Platform grant to GZ, the Canada Research Chair (CRC) program to GZ, Ontario Graduate Scholarship to AK, Ontario Trillium Scholarship to KY and

1 National Sciences and Engineering Research Council (NSERC) support to EW, PR and GZ.  
2 Special thanks go to Janet Fleites Medina for the dedicated husbandry of the zebrafish colony.  
3

#### 4 **Conflict of Interest**

5 The authors do not claim any conflict of interest.  
6

#### 7 **References**

- 8 [1] J. R. Fetcho and K. S. Liu, *Ann. N. Y. Acad. Sci.* **1998**, 860, 333.  
9 [2] K. Howe and A. Et, *Nature* **2013**, 496, 498.  
10 [3] V. Surendra, U. Raj Sharma and D. Goli, *Int. J. Pharmagenes.* **2011**, 2, 75.  
11 [4] F. M. Richards, W. K. Alderton, G. M. Kimber, Z. Liu, I. Strang, W. S. Redfern, J. P.  
12 Valentin, M. J. Winter and T. H. Hutchinson, *J. Pharmacol. Toxicol. Methods* **2008**, 58,  
13 50.  
14 [5] A. V. Kalueff and J. M. Cachat, *Zebrafish Models in Neurobehavioral Research*, Humana  
15 Press, illustrate. **2011**.  
16 [6] Y. Xi, S. Noble and M. Ekker, *Curr. Neurol. Neurosci. Rep.* **2011**, 11, 274.  
17 [7] D. S. Wiley, S. E. Redfield and L. I. Zon, *Methods Cell Biol.* **2017**, 46, 651.  
18 [8] J. Akagi, C. J. Hall, K. E. Crosier, P. S. Crosier and D. Wlodkowic **2013**, 892346.  
19 [9] W. F. An and N. Tolliday, *Mol. Biotechnol.* **2010**, 45, 180.  
20 [10] A. Khalili and P. Rezai, *Briefings Funct. Genomics* **2019**, 1.  
21 [11] F. Yang, C. Gao, P. Wang, G. J. Zhang and Z. Chen, *Lab Chip* **2016**, 16, 1106.  
22 [12] C. Y. Chen and C. M. Cheng, *Adv. Healthc. Mater.* **2014**, 3, 940.  
23 [13] A. Nady, A. R. Peimani, G. Zoidl and P. Rezai, *Lab Chip* **2017**, 17, 4048.

- 1 [14] A. Khalili, A. R. Peimani, N. Safarian, K. Youssef, G. Zoidl and P. Rezai, *Integr. Biol.*  
2 **2019**, *11*, 373.
- 3 [15] X. Lin, S. Wang, X. Yu, Z. Liu, F. Wang, W. T. Li, S. H. Cheng, Q. Dai and P. Shi, *Lab*  
4 *Chip* **2015**, *15*, 680.
- 5 [16] X. Lin, V. W. T. Li, S. Chen, C. Y. Chan, S. H. Cheng and P. Shi, *Biomicrofluidics*, ,  
6 DOI:10.1063/1.4946013.
- 7 [17] M. Erickstad, L. A. Hale, S. H. Chalasani and A. Groisman, *Lab Chip* **2015**, *15*, 857.
- 8 [18] A. R. Peimani, G. Zoidl and P. Rezai, *Biomed. Microdevices* **2017**, *19*, 1.
- 9 [19] K. Mani, Y. C. Hsieh, B. Panigrahi and C. Y. Chen, *Biomicrofluidics* **2018**, *12*, 1.
- 10 [20] P. Rezai, A. Siddiqui, P. R. Selvaganapathy and B. P. Gupta, *Lab Chip* **2010**, *10*, 220.
- 11 [21] A. R. Peimani, G. Zoidl and P. Rezai, *Biomicrofluidics* **2018**, *12*, 1.
- 12 [22] A. R. Peimani, G. Zoidl and P. Rezai, *Biomicrofluidics*, , DOI:10.1063/1.5016381.
- 13 [23] S. Mondal, S. Ahlawat and S. P. Koushika, *J. Vis. Exp.* **2012**, 1.
- 14 [24] A. K. Gerhart and D. M. Janz, *Toxics*, , DOI:10.3390/toxics7030044.
- 15 [25] C. Pardo-Martin, T. Y. Chang, A. Allalou, C. Wählby and M. F. Yanik, *15th Int. Conf.*  
16 *Miniaturized Syst. Chem. Life Sci. 2011, MicroTAS 2011* **2011**, *3*, 1557.
- 17 [26] R. E. Ulanowicz, *Fish. energy Prod. a Symp.* **1976**, *1*, 77.
- 18 [27] R. P. Morgan, R. E. Ulanowicz, V. J. Rasin, L. A. Noe and G. B. Gray, *Trans. Am. Fish.*  
19 *Soc.* **1976**, *105*, 149.
- 20 [28] A. Khalili, E. van Wijngaarden, G. R. Zoidl and P. Rezai, *Sensors Actuators A. Phys.*